20 June 1969, Volume 164, Number 3886 **SCIENCE**

High-Temperature Batteries

Research in high-temperature electrochemistry reveals compact, powerful energy-storage cells.

E. J. Cairns and H. Shimotake

In our technologically oriented society, there is an increasing need for an array of compact, convenient, pollution-free electrical power sources and energy-storage devices. A large number of power-source needs, both civilian and military, have remained unfulfilled because of the limited capabilities of presently available batteries and engine generators. In an attempt to satisfy these needs, a great deal of effort has been expended in the last decade in the development of devices for energy conversion and energy storage. A large portion of the effort has been devoted to electrochemical devices such as fuel cells (*1*), metal|air cells (*2*), secondary (electrically rechargeable) cells with both aqueous (*3, 4*) and nonaqueous (*5*) electrolytes, and thermally regenerative cells (*6*).

Because of the proliferation in types and names of electrochemical cells, we have summarized in Table 1 the types of cells presently receiving attention, their commonly accepted names, and examples of each type. The classification of electrochemical cells is simplified if it is remembered that the cell is merely a converter of energy; the type of cell can be designated according to the source of the energy that is being converted.

A fuel cell continuously converts the Gibbs free energy of combustion of a conventional fuel to electrical energy as long as fuel is supplied. In many fuel cells, the anode reactant (fuel) is gaseous; it reacts at a porous, catalyzed anode, yielding CO_2 or H_2O, or both, as the reaction products. By definition, the cathode reactant is oxygen (preferably from air), which is reduced at a porous, catalyzed cathode. The electrolyte must not participate in the net cell reaction; that is, it must remain invariant.

Primary cells may be self-contained like the Leclanché cell (*7*) (for example, a flashlight cell), continuous-feed like the lithium|chlorine primary cell (*8*), or so-called mechanically rechargeable, where the anodes and electrolyte are manually replaced after they are consumed. Examples of this type are the zinc|air (*9*) and magnesium|air cells (*10*).

If the electrochemical reactions of a discharged cell can be reversed by reversal of the direction of the current flow and if the electrodes and electrolyte are returned to their original conditions by this process, the cell can operate as an energy-storage device called a secondary cell. In practice, some room-temperature secondary cells can remain useful for thousands of charge-discharge cycles, if the cycles are properly performed (slow charge and only partial discharge).

If thermal energy is the energy source for an electrochemical system, then the cell is called a thermally regenerative cell. This type of cell is generally composed of a simple evaporator (or boiler), which continuously separates the products of the cell reaction at a relatively high temperature, and an electrochemical cell, which operates at a lower temperature. This system is a heat engine in the thermodynamic sense; therefore its efficiency is limited by the efficiency of the Carnot cycle.

Although a wide variety of electrochemical cells is available, none of these can deliver enough power per unit weight (specific power in watt/kg) and store enough energy per unit weight (specific energy in watt-hour/kg) to make them useful in such demanding applications as long-lived power supplies for spacecraft, certain military communications, vehicle propulsion (both military and civilian), and off-peak energy storage for central stations. Generally, the accepted criteria for such applications have been a specific power of 220 watt/kg and a specific energy of 220 watt-hour/kg. Special nickel-cadmium ($Cd|KOH|Ni_2O_3$) and silver-zinc ($Zn|KOH|AgO$) cells can deliver 220 watt/kg, but no other cells, including fuel cells, can meet this requirement. No available secondary cells can meet the specific energy requirement of 220 watt-hour/kg, but some fuel-cell systems can exceed it.

New Electrochemical Cells

As it became clear that no electrochemical cells being investigated a few years ago could meet the requirements of both specific energy and specific power, some new investigations were initiated with the goal of achieving 220 watt-hour/kg and 220 watt/kg. Some of the characteristics considered in the search for high-performance electrochemical cells are shown in Table 2. The characteristics that primarily affect the specific energy are electronegativity and equivalent weight. The elements having the lowest electronegativity are those of groups I A and II A of the periodic table, that is, the alkali and alkaline-earth metals; their low electro-

---

The authors are members of the Chemical Engineering Division, Argonne National Laboratory, Argonne, Illinois; Dr. Cairns is leader of the energy conversion group.

Table 1. Types of electrochemical cells. Fuel cells use conventional fuel and oxygen as the energy source; primary cells use energy supplied by the anode and cathode reactants; secondary cells use electricity; thermally regenerative cells use thermal energy.

System	Name
	Fuel cell
N_2H_4|KOH(aq)|air	Hydrazine fuel cell (*28*)
	Primary cell
Zn|NH_4Cl(aq)|MnO_2	Leclanché cell (dry cell) (*7*)
Zn|KOH(aq)|O_2	Zinc|oxygen primary cell (*29*)
Li|LiCl(liq)|Cl_2	Lithium|chlorine primary cell (*8*)
	Secondary cell
Pb|H_2SO_4(aq)|PbO_2	Lead-acid cell (*3*)
Cd|KOH(aq)|Ni_2O_3	Nickel-cadmium cell (*30*)
Zn|KOH(aq)|AgO	Silver-zinc cell (*31*)
Zn|KOH(aq)|air	Zinc|air secondary cell (*9*)
Li|KPF_6(nonaq)|CuF_2	Lithium|copper fluoride cell (*32*)
	Thermally regenerative cell
Li|LiX(liq)|Sn	Lithium|tin thermally regenerative cell (*6*)

negativity makes them most suitable for use as anode materials because they surrender their electrons more easily than other elements. Conversely, the elements with the highest electronegativities are most suitable as cathode materials because they have the greatest affinity for electrons; these elements are found in groups VI A and VII A, the chalcogens and halogens. The large difference of electronegativities between anode and cathode materials provides a relatively large cell voltage (in the range of 2 to 4 volts). Selection of the anode (groups I A and II A) and cathode (groups VI A and VII A) materials from those elements of lowest equivalent weight (those high up on the periodic table) yields the lightest-weight combination of reactants, corresponding to a high specific energy.

The effect of electronegativity difference (as reflected by the cell voltage) and equivalent weight (of anode material plus cathode material) on the maximum theoretical specific energy is shown in Fig. 1 for several systems of interest. Alkali metal|fluorine cells are not shown because no work has been reported and because they would probably have to operate at unattractively high temperatures (at least 850°C for Li|F_2 and 1000°C for Na|F_2). Because of the high electronegativity of fluorine, the Li|F_2 cell has an electromotive force of 5.2 volts; the Na|F_2 cell has an electromotive force of 4.5 volts. The interhalogens may be interesting cathode reactants, but they have not yet been investigated. In Fig. 1 the specific energy has been calculated on the basis of the weights of reactants only. It is not possible to realize these specific energy values in practice because the weights of electrolyte, cell housing, and terminals must be included in the calculation of the specific energy of a practical cell. When this is done, the specific energy values are lowered by a factor of three to six, depending on the cell design. There are thus several systems in Fig. 1 that may reasonably be expected to yield over 220 watt-hour/kg, such as Li|S, Li|Cl_2, Li|Se, and Na|S.

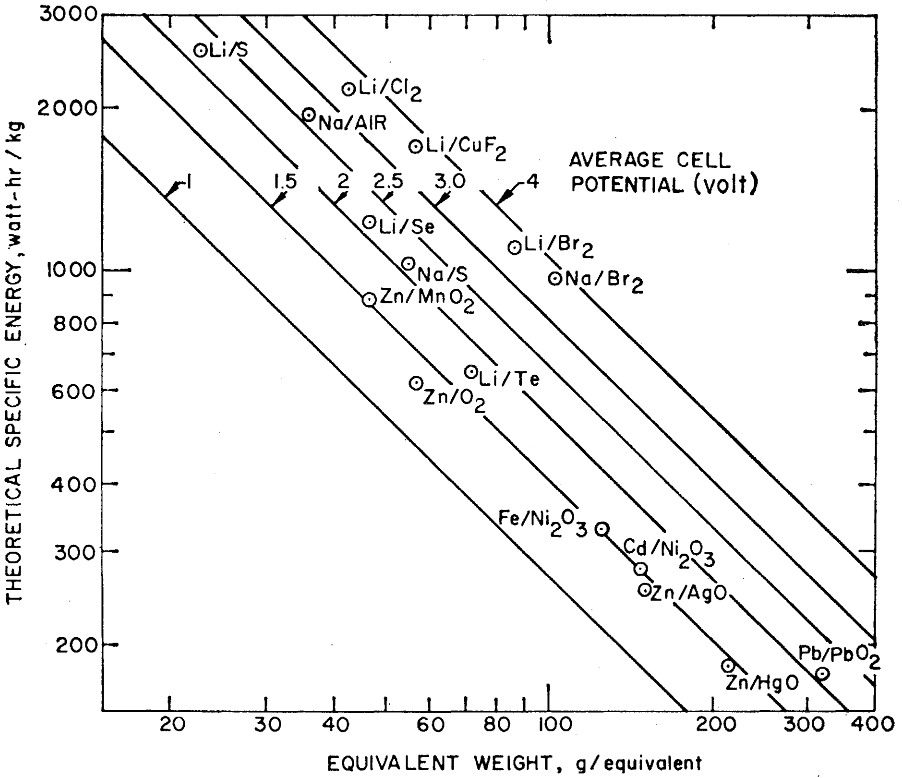

Fig. 1. Effect of electronegativity difference between anode and cathode (as reflected by the cell voltage) and of equivalent weight (of anode plus cathode materials) on the maximum theoretical specific energy of various electrochemical cells.

In order to maximize the specific power of an electrochemical cell, the electronic and electrolytic resistances of the cell must be minimized. This can be done by selecting materials of high conductivity and by optimizing the cell design (by use of short conduction paths and small interelectrode distances). The largest contribution to the internal resistance of electrochemical cells is usually made by the electrolyte, and it is necessary to minimize the electrolyte resistance. Fused-salt electrolytes have far lower resistivities than electrolytes that use aqueous or organic solvents (*5*). In order to use fused-salt electrolytes, one must suffer the inconvenience of operating the cell at temperatures above the melting point of the salts (usually well above 100°C and sometimes as high as 650°C). The elevated temperatures required for the use of fused-salt electrolytes have the advantages of increasing the exchange-current densities (rates of the electrode reactions) and allowing the use of liquid-metal electrodes. Many liquid-metal electrodes have exchange-current densities of several amperes per square centimeter of electrode area, as compared to 10^{-3} ampere/cm^2 for hydrogen and 10^{-9} ampere/cm^2 for oxygen electrodes at room temperature. Therefore, the combination of fused-salt electrolytes and liquid electrodes at elevated temperatures is expected to yield high specific power.

Within the last few years, several

laboratories have reported research on prototype cells with fused-salt electrolytes that are expected to have specific energies above 220 watt-hour/kg when produced in practical configurations. These systems are still in the research-and-development stages; some of their characteristics are summarized in Table 3. All of the cells listed operate above 100°C and use liquid lithium or liquid sodium as the anode. All of the cells except one (Na|S) have fused-salt electrolytes. The specific energies expected for these systems when reasonable battery designs are used are all above 220 watt-hour/kg and the specific powers are above 220 watt/kg, except for the specific power of the Na|air cell. These values are in sharp contrast to the specific-energy values of 20 to 120 watt-hour/kg for all of the cells of Table 1, except for lithium|metal halide cells, which have a specific energy of 200 watt-hour/kg but a specific power of only 40 to 45 watt/kg.

There have been several novel approaches in the development of the new high-temperature cells listed in Table 3, each of which is discussed below. The strong points and problem areas of each will be noted before possible applications are considered.

Table 2. Characteristics for high-performance electrochemical cells.

Characteristics	Anode reactant	Cathode reactant	Electrolyte
Electronegativity	Low	High	
Equivalent weight	Low	Low	Low
Conductivity	High	High	High
Electrochemical reaction rate (exchange-current density	High	High	High
Solubility in electrolyte	Low	Low	

Lithium | Chlorine Cell

The lithium|chlorine cell, the first of these new cells reported (*8*), has received the largest expenditure for research and development. It has the highest cell voltage (3.46 volts) and the highest operating temperature (650°C). The cell, shown schematically in Fig. 2a, consists of a porous, stainless steel, fiber metal wick designed to contain and transport the liquid lithium (by capillary action), a molten lithium chloride electrolyte (melting point 609°C), and a porous carbon cathode at which chlorine reacts. The lithium reactant and the lithium chloride reaction product are stored within the cell, whereas the chlorine is fed to the cell from external storage. The reaction at the anode is

$$\mathrm{Li} \rightarrow \mathrm{Li}^+ + e^- \tag{1a}$$

and at the cathode is

$$\tfrac{1}{2}\ \mathrm{Cl}_2 + e^- \rightarrow \mathrm{Cl}^- \tag{1b}$$

The liquid lithium anode is capable of very high current densities and shows no measurable overvoltage up to 40 ampere/cm^2 (*8*). The LiCl electrolyte is the product of the cell reaction, thus eliminating the possibility of any diffusion limitation caused by migration of reaction products away from the reaction sites. The resistivity of the electrolyte is only 0.17 ohm-cm (*11*), but a major portion of the cell resistance is due to the electrolyte. The electrode reaction at the chlorine cathode is not as fast as that at the lithium anode. The exchange-current density is about 0.2 ampere/cm^2, which indicates that a voltage loss of about 0.2 volt, attributable to the cathode reaction, may be expected at current densities near 3 ampere/cm^2 (*12, 13*). In addition, there is a resistive loss in the porous carbon. Perhaps the most bothersome source of voltage loss in this cell is that caused by the accumulation of inert impurities from the chlorine in the pores of the cathode. These impurities (for example, CO_2 and N_2) present a diffusion barrier to the incoming chlorine and cause a diffusion limitation that shows up as a limiting current density that cannot be exceeded. The magnitude of the limiting current density is a function of the purity of the chlorine and the structure of the porous carbon electrode (*14*). With optimum pore sizes (average diameter is 0.6 micron) and thin electrodes (0.1 cm), a limiting current density of about 10 ampere/cm^2 can be achieved at a chlorine pressure of 3 atm (*12*). It is helpful to "sweep out" the cathode with an excess flow of Cl_2 (5 or 10 percent) to minimize the accumulation of impurities.

Even with the limitations just discussed, a maximum power density of 40 watt/cm^2 has been achieved for periods of 20 minutes when the cell design has been optimized for discharge operation only (*12*). This probably

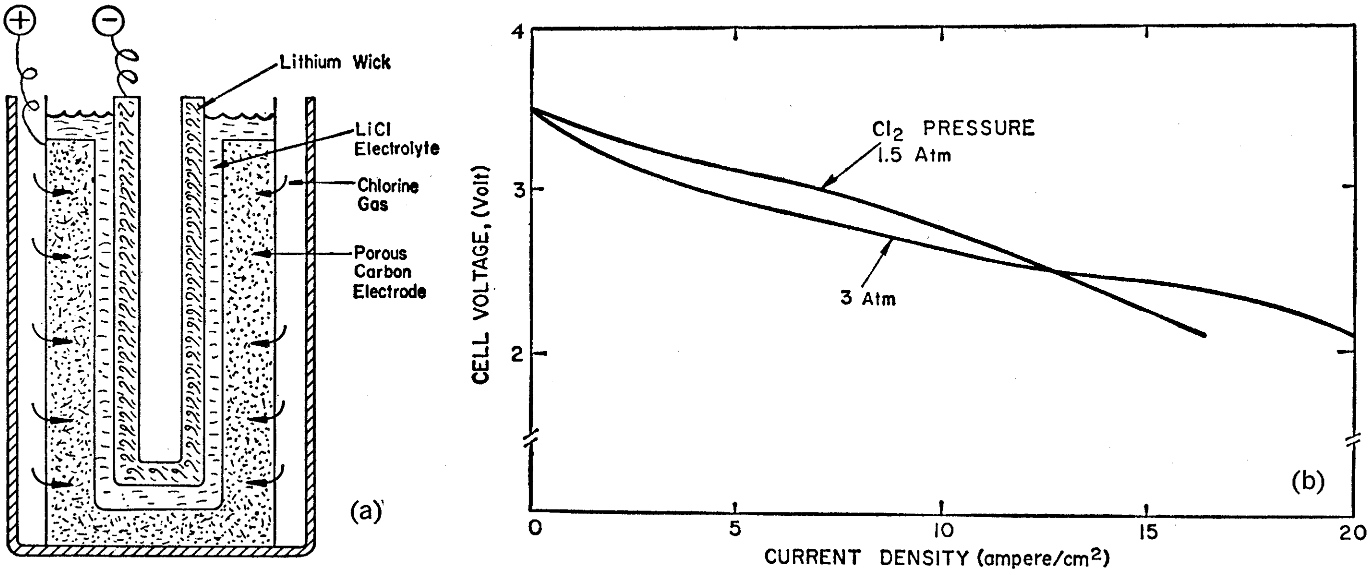

Fig. 2. (a) Schematic diagram of a lithium | chlorine cell. (b) Typical voltage-current density curves for a lithium | chlorine primary cell (*12*). Cell temperature is 680°C; interelectrode distance is 0.1 cm.

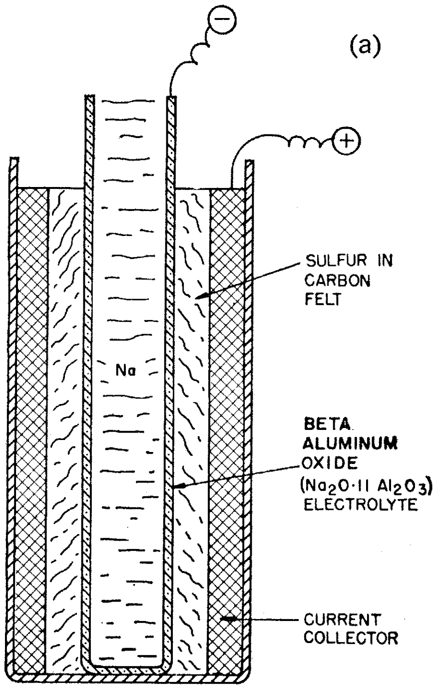

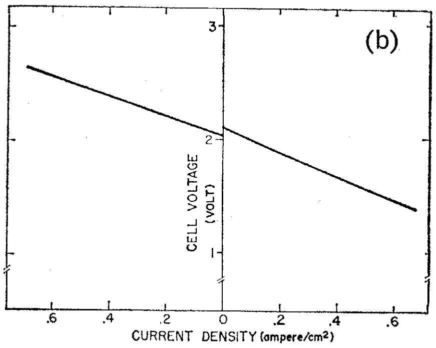

Fig. 3. (a) Schematic diagram of a sodium | sulfur cell. (b) Voltage–current density curves for charge and discharge for a sodium | sulfur cell (*18*). Cell temperature is 300°C; interelectrode distance is 0.07 cm.

represents the highest power density ever reported for an electrochemical device. Two typical voltage–current density curves for a Li|Cl_2 primary cell are shown in Fig. 2b (*12*). The modest deviation from linearity shown by the curves in Fig. 2b is an indication of the small magnitude of the voltage losses due to diffusion or to slow electrochemical reactions in the current-density range shown. The important losses of voltage are resistive in nature, primarily assignable to the electrolyte and the carbon cathode.

The admirable performance of the Li|Cl_2 cell is accompanied by some disadvantages associated with the necessities of recharge and long life. During recharge, the electrolysis products (liquid lithium and gaseous chlorine) must be liberated in such a manner that they are easily separated and stored. This can be accomplished at some cost of performance (as a result of increased internal resistance) by the use of special electrodes which have porous, electronically insulating layers on the sides facing the electrolyte; where these layers are wetted by the electrolyte, they form a seal that prevents the escape of electrolysis products from the porous electrodes. This type of structure, called a valve electrode, has been tested in the Li|Cl_2 cell (*15*).

The stability of the materials of construction, especially insulators, toward lithium, chlorine, and lithium chloride, is the main factor which determines the life of this cell. Molten lithium attacks almost all known insulators. Beryllium oxide has been used successfully but only for about an hour; the binding agent used in sintering the BeO is attacked, causing the insulators to disintegrate (*16*). It may be possible to use lithium aluminate as an insulator (*16*). It is absolutely necessary to keep the lithium away from the carbon cathode (an interlamellar attack takes place) and the chlorine away from the stainless steel cell parts, because these combinations are reactive. The high temperature and elevated chlorine pressure promote self-discharge by diffusion of reactants (particularly lithium) through the electrolyte.

Much effort has been devoted to design calculations and performance estimations for fully engineered Li|Cl_2 batteries. For short-discharge applications in the primary mode (no electrical recharge), these batteries are expected to deliver about 1000 watt/kg and 400 watt-hour/kg of system (including reactant storage). For longer-term operation, it may be more desirable to operate at somewhat lower specific power (600 watt/kg), which permits the use of lower-purity Cl_2 and is conducive to longer cell life.

A second version of the Li|Cl_2 cell (*17*) stores the chlorine within the cell by adsorption on the carbon cathode which has a high specific area (about 1000 m^2/g); the lithium is stored in the form of a solid lithium-aluminum alloy. Electrodes of this type allow the cell to be completely sealed. The Cl_2 adsorption capacity of the carbon cathode presently limits the specific energy of this cell to about 70 watt-hour/kg.

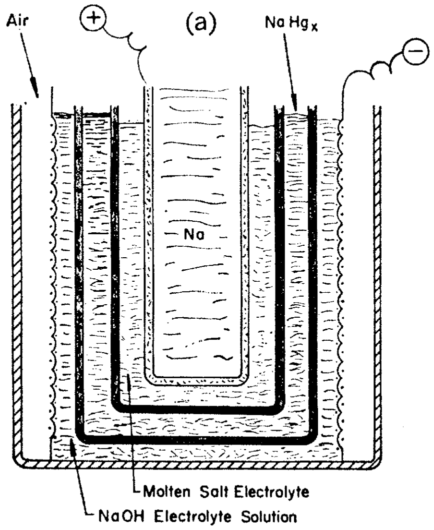

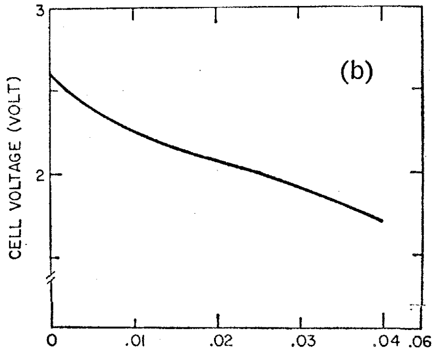

Fig. 4. (a) Schematic diagram of a sodium | air cell. (b) Typical voltage–current density curve for a sodium | air cell (*19*). Cell temperature is 135°C.

Sodium | Sulfur Cell

The sodium|sulfur cell is the only one discussed here that does not have a fused-salt electrolyte; it has instead a solid sodium-ion conductor called beta aluminum oxide ($Na_2O \cdot 11Al_2O_3$) (*18*). This electrolyte has the mechanical properties of a ceramic, and its crystals can conduct sodium ions along planes in its lamellar structure. It is therefore desirable to orient the crystals of beta aluminum oxide so that the conducting direction is perpendicular to the interface between the electrode and electrolyte. The resistivity of the modified beta aluminum oxide used as the electrolyte in this cell is about 5 ohm-cm at 300°C (*18*).

The laboratory version of the sodium|sulfur cell is shown schematically in Fig. 3a. The pool of liquid sodium inside the tubular electrolyte is the anode. Since sulfur is not electronically conducting, it is necessary to provide current collection at the cathode in the form of carbon felt placed around the electrolyte. The liquid sulfur is held in the carbon felt by capillary forces. The reaction of the anode is

$$x\mathrm{Na} \rightarrow x\mathrm{Na}^+ + xe^- \qquad (2a)$$

and at the cathode is

$$x\mathrm{Na}^+ + xe^- + y\mathrm{S} \rightarrow \mathrm{Na}_x\mathrm{S}_y \qquad (2b)$$

The sodium polysulfides (Na_2S_5, Na_2S_4, Na_2S_2) formed at the cathode are not miscible with sulfur at the temperature of cell operation (about 300°C) but they are semiconducting; thus the cathode reaction can proceed as the products accumulate.

The voltage–current density curves for charge and discharge are shown in Fig. 3b (*18*). The fact that these curves are essentially straight lines may be taken as evidence that no significant overvoltages caused by electrochemical reactions or slow mass transport occur at current densities up to 0.68 ampere/cm^2 (*18*). The slope of the curves is equal to the internal resistance of the cell corresponding to 1 cm^2 of electrolyte.

The materials problems for sodium and sulfur at 300°C are much less severe than those for the Li|Cl$_2$ cell. The electrolyte consisting of beta aluminum oxide is not attacked by sodium or sulfur, and there is almost no chance for a significant rate of self-discharge by diffusion of reactants through the electrolyte. It must be acknowledged, however, that ceramic materials are sensitive to mechanical shock and sometimes to thermal shock and thermal cycling. Stainless steels will probably be appropriate as metals of construction, and carbon will probably be stable as the cathode current collector. The relatively high resistivity of beta aluminum oxide limits this cell to modest current densities (less than 1 ampere/cm^2).

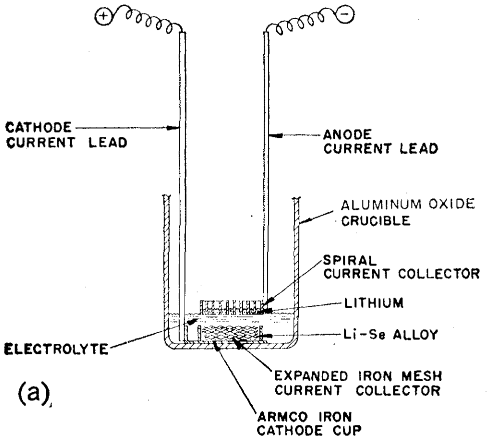

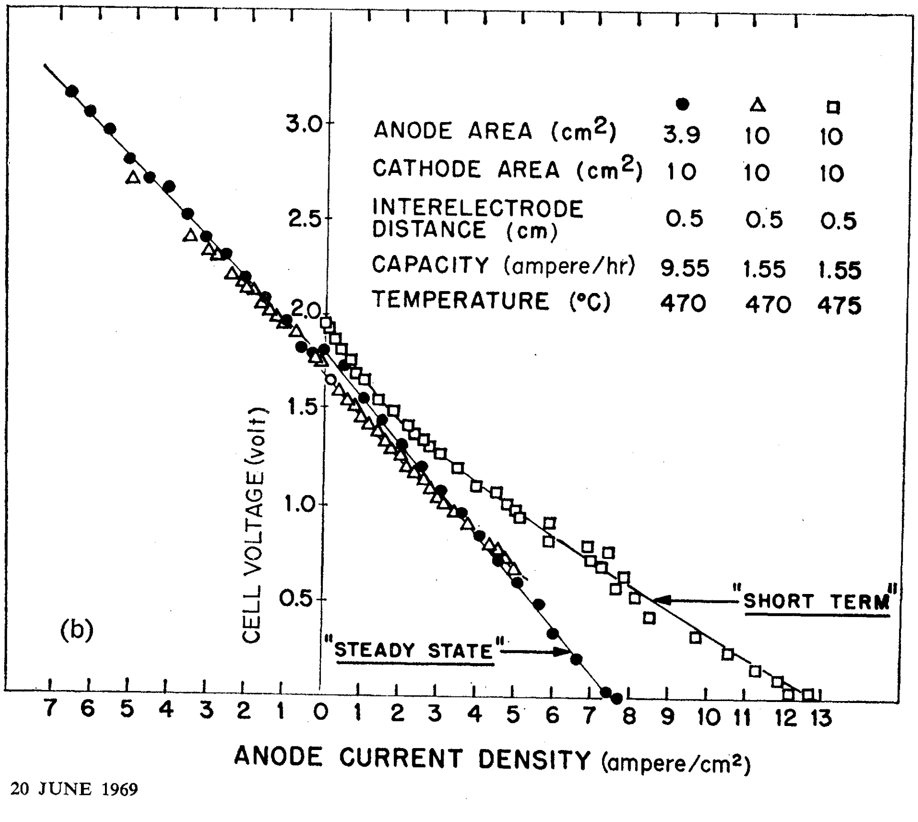

Fig. 5. (a) Schematic diagram of a typical lithium | chalcogen cell for use with a liquid LiF-LiCl·LiI eutectic electrolyte. (b) Two voltage–current density curves for a lithium | tellurium cell.

Sodium | Air Cell

The sodium|air cell (*19*) is actually two cells connected electrically and electrochemically in series; the arrangement may be represented as

$$\mathrm{Na}|\mathrm{Na}^+ \text{ fused salt}|\mathrm{NaHg}_x|\mathrm{NaOH}_{\mathrm{aq}}|(\mathrm{Pt}) \text{ air} \qquad (3)$$

In the first cell, the reaction at the anode is

$$\mathrm{Na} \rightarrow \mathrm{Na}^+ + e^- \qquad (4a)$$

and at the cathode is

$$\mathrm{Na}^+ + e^- + x\mathrm{Hg} \rightarrow \mathrm{NaHg}_x \qquad (4b)$$

Proceeding at the same rate, the reaction in the second cell at the anode is

$$\mathrm{NaHg}_x \rightarrow \mathrm{Na}^+ + e^- + x\mathrm{Hg} \qquad (5a)$$

and at the cathode is

$$\tfrac{1}{4}\ \mathrm{O}_2\ (\text{air}) + \tfrac{1}{2}\ \mathrm{H_2O} + e^- \rightarrow \mathrm{OH}^- \qquad (5b)$$

The overall cell reaction is the production of aqueous sodium hydroxide from sodium, water (in the aqueous electrolyte), and oxygen from air. It is not possible to carry out the direct electrochemical combination of pure sodium with water and oxygen because the sodium would react chemically with the water, producing little or no electricity.

The most recently reported sodium|air cell (*19*) consists of two liquid sodium electrodes contained in porous tubes that are penetrated by the sodium-ion fused-salt electrolyte. The cell is shown schematically in Fig. 4a. The amalgam electrode is supported on a fine-mesh metal screen with the amalgam held in place by capillary forces. The amalgam electrode also keeps the fused-salt electrolyte and the aqueous NaOH electrolyte [50 to 70 percent (by weight) NaOH] separated. The air cathodes are polytetrafluoroethylene-bonded porous electrodes containing platinum black at a loading of 9 mg/cm^2.

The current density–voltage curve for this cell is shown in Fig. 4b. The operating temperature is 135°C, just above the melting point of the fused-salt electrolyte of proprietary composition. The current densities available from this cell are much lower than those of any other cell discussed here. The process that is responsible for limiting the current density is the diffusion of sodium through the sodium amalgam electrode. The overvoltage is highest on the fused-salt side of this electrode, and a limiting current density of slightly more than 0.04 ampere/cm^2 is observed (*19*). Recently, a flowing amalgam electrode has been used in this cell which results in an increase of the limiting current density to about 0.160 ampere/cm^2; the slow step is still at the interface between the fused salt and the amalgam. The voltage loss at the nonflowing amalgam electrode is about 0.40 volt at 0.040 ampere/cm^2. The air electrode has an overvoltage of about 0.25 volt at the same current density. The life of the air cathode at 135°C is short.

In order to avoid the difficulties associated with operating the air cathode at an elevated temperature and the relatively low limiting current densities at the interface between the fused salt and the amalgam, it may be worthwhile to eliminate the portion of the dual cell consisting of $Na|Na^+$ fused salt$|NaHg_x$ at a loss of only about 0.7 volt. The resulting sodium amalgam|air cell would then compete with other low-temperature secondary cells such as $Cd|Ni_2O_3$, $Zn|Ag_2O$, and Zn|air.

Lithium|Chalcogen Cells

Lithium|chalcogen cells with fused-salt (lithium halide) electrolytes which use tellurium (*20*), selenium (*21*), and sulfur (*22*) have been investigated as the cathode materials. Since the electronegativity increases in the order Te, Se, S, the cell voltages increase in the same order. Typical open-circuit voltages for these cells in the charged condition are 1.75, 2.2, and 2.4 volts, respectively. The specific energies of these cells increase in the order listed to a larger extent than the cell voltages because the atomic weights of the cathode materials decrease in the order 127.6, 78.96, and 32.06. The specific powers

Table 3. Characteristics of some high-temperature batteries.

System	Voltage (volts)	Theoretical specific energy (watt-hour/kg)	Temp. (°C)	Expected specific energy (watt-hour/kg)	Expected specific power (watt/kg)	Demonstrated		
						Power density (watt/cm^2)	Charge rate (hour)	Life (hour)
$Li|LiCl|Cl_2$ (*12*)	3.5	2180	680	330–400	1000–1200	20	—	< 1
$Li|LiCl|Cl_2$ (*17*)	3.4	2120	500*	110–165	330–440	4	< 0.17	2200
$Na|Na_2O \cdot 11Al_2O_3|S$ (*18*)	2.1	1030	300	180–330	330	0.85	~ 1	?
Na|NaX|Na + Hg|NaOH|air (*19*)	2.6	1940	135	180–275	100	.28	> 10	200
Li|LiF-LiCl-LiI|Te (*20*)	1.7	612	470	185–265	550–800	5	< 0.25	160
Li|LiF-LiCl-LiI|Se (*21*)	2.1	1210	365	220–330	600–1000	6	< .25	160
Li|LiCl-LiI-KI|S (*22*)	2.3	2680	347	250–360	550–800	4	< .5	8

* For some $Li|Cl_2$ cells, operating temperatures below 500°C have been reported (*17*).

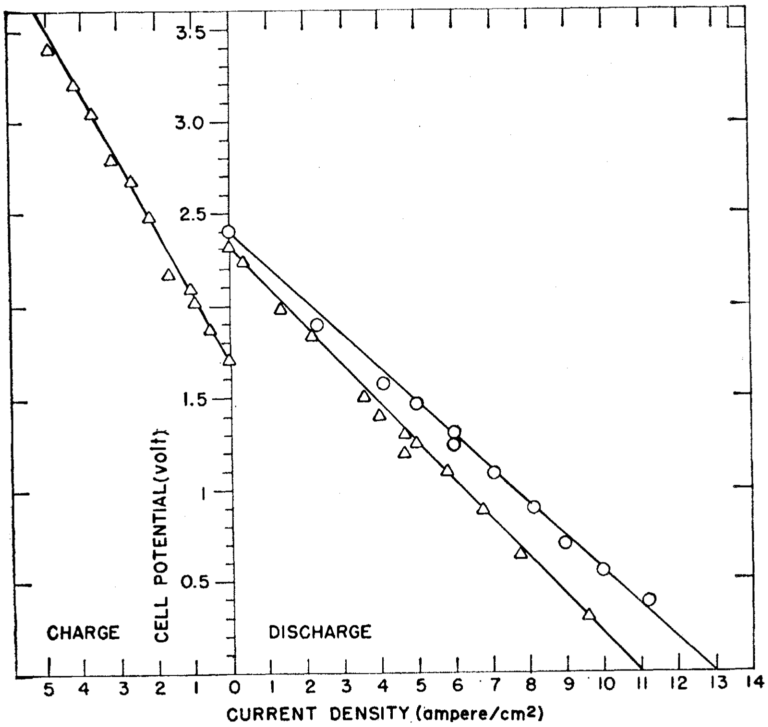

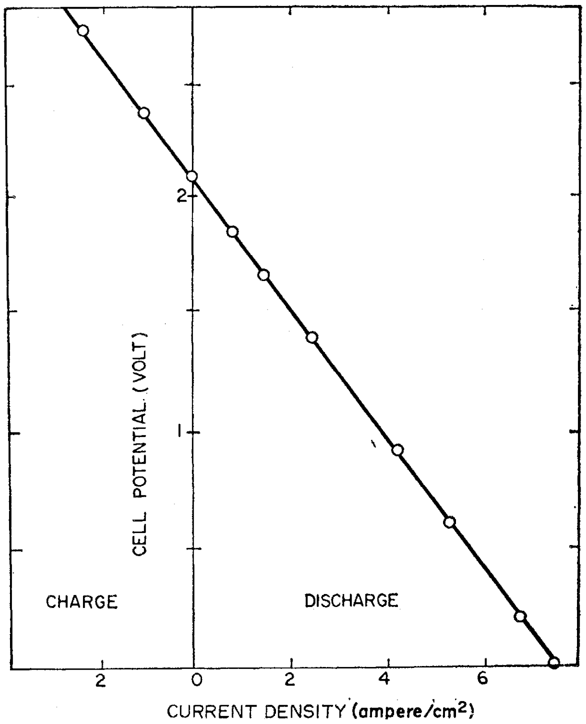

Fig. 6 (left). Voltage–current density curves for a lithium|selenium cell with a LiF-LiCl-LiI eutectic electrolyte, a stainless steel spiral anode, and an expanded iron mesh cathode current collector. Anode area is 10 cm^2; cathode area is 10 cm^2; interelectrode distance is 0.5 cm; capacity ≈ 6 ampere hours; temperature is 375°C; ○, short-time data; △, steady-state data. Fig. 7 (right). Short-term voltage–current density curve for charge and discharge for a lithium|sulfur cell with a LiCl-LiI-KI electrolyte. Anode area is 10 cm^2; cathode area is 10 cm^2; interelectrode distance is 0.5 cm; temperature is 347°C.

of these cells do not necessarily follow the same order because the electronic resistivities of the chalcogens and their alloys with lithium increase in the order Te, Se, S. This means that the current collection (or electron distribution) at the cathode becomes more difficult in the order Te, Se, S. The higher resistance of the cathode causes the internal resistance of the cell to increase (for a given design), resulting in lower power output. The melting points of the chalcogens are: tellurium, 449.8°C; selenium, 220°C; sulfur, 118°C; thus cell operating temperatures of at least these values are required.

A typical lithium|chalcogen laboratory cell for use with a liquid electrolyte is shown in Fig. 5a. Two voltage–current density curves for this cell operating at 470°C with a tellurium cathode utilizing a simple current collector with a single annular fin are shown in Fig. 5b. The "short-term" curve represents the performance that can be obtained at nearly full charge (about 5 atom percent Li in Te), whereas the "steady-state" curve corresponds to the voltage plateau that appears when cell voltage is plotted against percent discharge (20 to 30 atom percent Li in Te). The maximum power density at steady state is 3.5 watt/cm^2; at short term the maximum power density is 5 watt/cm^2. The charging portions of the voltage–current density curves show that the Li|Te cell can be recharged at very high current densities.

When selenium was substituted for tellurium in this cell, the performance was rather poor, only 1 ampere/cm^2 at short circuit, because of the relatively high resistivity of liquid selenium. After a network of expanded iron mesh was added to the cathode to improve the current collection, the cell performance improved, yielding the curves shown in Fig. 6. The maximum steady-state power density was 6 watt/cm^2, achieved at 365°C rather than 470°C and with a lower cell weight (the weight of iron mesh added to the cathode was about 20 percent of the weight of the selenium).

The encouraging results with the Li|Se cell prompted experiments with a Li|S cell of the same design. The performance of the Li|S cell was not as steady as that of the Li|Te or Li|Se cells, and the internal resistance of the cell increased with the accumulation of lithium sulfides in the cathode. The short-term voltage–current density data are shown in Fig. 7. The maximum power density was 4 watt/cm^2 at 347°C. Efficient current collection at the sulfur cathode is presently being studied.

The three-liquid cell of Fig. 5a is not practical for portable or transportable applications, where the cell will be jostled and tipped. It is necessary to immobilize at least one of the liquid phases to make the cell position-insensitive. We have chosen to immobilize the fused-salt electrolyte in the form of a stiff paste by mixing it with a finely divided (0.1 micron in diameter) powder such as lithium aluminate in a 1:1 weight ratio. The paste electrolyte can be hot-pressed in molds to form the desired shapes, which are mechanically stable under the normal stresses encountered in these cells. The paste electrolyte has a continuous molten-salt phase, and the strength of the paste is due to the surface tension of the electrolyte in the fine-pore network formed by the inert ceramic powder. The force of surface tension per unit area ψ, which holds the paste together, is

$$\psi = 2\gamma \cos \theta / r \tag{6}$$

where γ is the surface tension of the electrolyte, θ is the contact angle between electrolyte and the inert ceramic powder (nearly 0° for good wetting), and r is the equivalent radius of the pores formed by the powder. The value of ψ is commonly in the range of tens

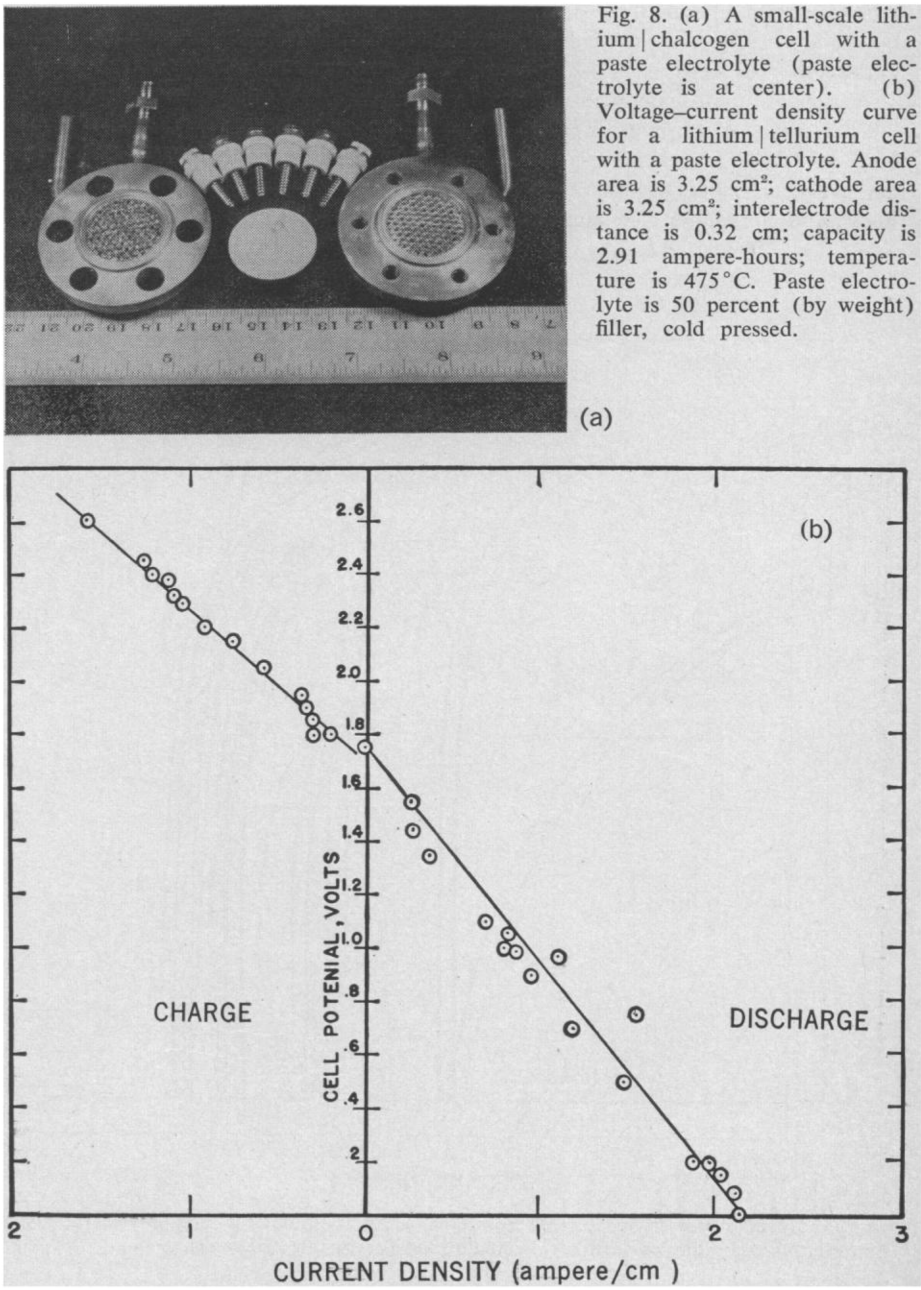

Fig. 8. (a) A small-scale lithium|chalcogen cell with a paste electrolyte (paste electrolyte is at center). (b) Voltage–current density curve for a lithium|tellurium cell with a paste electrolyte. Anode area is 3.25 cm^2; cathode area is 3.25 cm^2; interelectrode distance is 0.32 cm; capacity is 2.91 ampere-hours; temperature is 475°C. Paste electrolyte is 50 percent (by weight) filler, cold pressed.

Table 4. Comparison of various electric power sources for an urban automobile; vehicle weight: 900 kg; power source weight: 180 kg. According to a typical urban driving profile, 15 percent of the energy is used for acceleration and 85 percent for cruising. The required specific power of the system under peak load is 128 watt/kg, and the required specific power for cruising is 37.4 watt/kg.

System	Specific energy at peak load (watt-hour/kg)	Specific energy at normal load (watt-hour/kg)	Total energy (kilowatt-hour)	Range* (mile)	Recharging time (hour)
$\mathrm{Pb}\vert\mathrm{PbO_2}$	5.3	17.3	2.3	9	> 8
$\mathrm{Cd}\vert\mathrm{Ni_2O_3}$	44	53	5.0	19	> 8
$\mathrm{Zn}\vert\mathrm{AgO}$	124	144	25	95	> 8
$\mathrm{Na}\vert\mathrm{air}$	420	450	80	294	> 8
$\mathrm{Na}\vert\mathrm{S}$	254	330	54	205	1
$\mathrm{Li}\vert\mathrm{Cl_2}$	420	440	78	290	?
$\mathrm{Li}\vert\mathrm{Te}$	242	308	54	202	< 0.25
$\mathrm{Li}\vert\mathrm{Se}$	440	485	86	324	< 0.25
$\mathrm{Li}\vert\mathrm{S}$	340	345	62	229	< 0.25

* Under typical urban driving conditions, the energy requirement is 0.27 kilowatt-hour/mile.

of atmospheres. Minimization of the equivalent pore radius maximizes the strength of the paste. These paste electrolytes are similar to those introduced by Broers (*23*) and used in molten carbonate fuel cells (*24*).

A typical small-scale laboratory cell with a paste electrolyte is shown in Fig. 8a (*25*). The paste has some of the physical properties of a ceramic, but it also is capable of changing shape slightly under stress when the temperature is above the melting point of the electrolyte. The resistivity of the paste electrolyte depends upon the volume fraction of the filler and the conditions of preparation, but a representative value is two to four times the resistivity of the pure electrolyte (*6, 25*). The voltage–current density curve for a lithium|tellurium cell with a paste electrolyte is shown in Fig. 8b. Comparison of these results with those in Fig. 5b shows the effect of the increased resistivity of the paste on cell performance. It is likely that the short-circuit current density of the paste-electrolyte Li|Te cell can be increased to about 4 ampere/cm^2 by modest improvements in the paste electrolyte.

The energy storage capacity of lithium|chalcogen cells is determined by the amounts of lithium and chalcogen in the cells and their ratio. It is necessary to minimize the ratio of chalcogen to lithium in order to maximize the specific energy, but this ratio cannot exceed the value corresponding to the solidification of the cathode material at complete discharge. The solidification composition approaches that of the Li$_2$Y compound (where Y represents a chalcogen) so that 60 atom percent lithium may be regarded as a practical upper limit for the lithium content of the cathode.

The lithium|chalcogen secondary cells have power densities second only to those of the Li|Cl$_2$ primary cell. They operate at temperatures between those of the Na|air and Li|Cl$_2$ cells and have materials problems that are not as severe as those for the Li|Cl$_2$ cell but probably more severe than those of the Na|air cell.

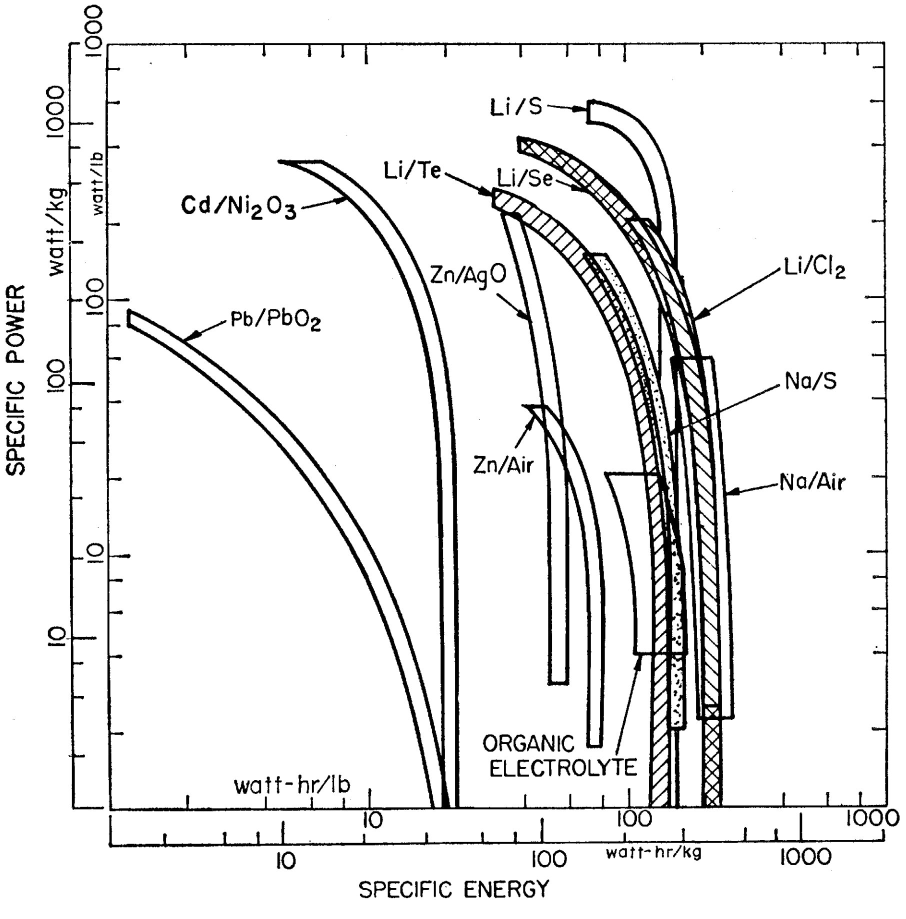

Fig. 9. Specific power–specific energy curves for commercial and high-temperature batteries used in the performance calculations for an electric auto.

Possible Applications and Outlook

If and when one or more of the secondary electrochemical cells discussed above is developed into a practical battery, what applications might it have? A number of possible applications, covering a wide range of energy and power, include: electrical power for spacecraft (watts to kilowatts); military communications and emergency power (kilowatts); materials-handling vehicles (kilowatts); military vehicles (tens to hundreds of kilowatts); boats and submarines (tens to hundreds of kilowatts); remote locations (kilowatts to tens of kilowatts); buses and trucks (hundreds of kilowatts); urban automobiles (tens of kilowatts); and off-peak energy storage for central stations (megawatts). These are arranged with applications of higher probability first. As one moves down the list, the probability of success decreases for both technical and economic reasons. Excluded from the list as being highly impractical are household appliances, flashlights, and other applications involving low power and a low duty-cycle.

The high-temperature batteries may be used either alone or in combination with some primary energy source (such as a fuel cell). Some advantages and applications of these so-called hybrid systems have been discussed (*26*). The greatest benefit of a hybrid system is obtained when the ratio of peak power demand to average power is quite high (5 or more).

To illustrate the potential superiority of high-temperature batteries in a familiar situation, we have calculated the performance of a small urban electric automobile under the conditions of an urban driving profile. The automobile is assumed to weigh 900 kg and to contain 180 kg of batteries. The auto must have at least the acceleration capabilities of a 1960 Volkswagen (peak power 23.2 kilowatts). The characteristics of the batteries used in these calculations are shown in Fig. 9. The curves for commercial batteries represent actual performance (*27*). The curves for the high-temperature batteries are estimates based on laboratory results and specific cell designs. The estimates for lithium|chalcogen cells were made by us, for Na|S cells by Weber and Kummer (*18*), for Li|Cl$_2$ cells by Hietbrink *et al.* (*12*), and for Na|air cells by Heredy *et al.* (*19*).

The results of calculations for the urban electric auto (Table 4) indicate that only the high-temperature batteries can be expected to provide the acceleration, range, and rapid recharge characteristics desirable for an urban vehicle of acceptable performance and convenience. In general, a range of 150 to 200 miles is considered to be a desirable objective, with longer ranges being an added convenience.

High-temperature batteries are still in the research and early development stages. Many problems remain to be solved, most notably those associated with the materials and life of the battery. Because of the limited experience with multicelled batteries, it can be expected that many difficult engineering problems will emerge. The problems of maintaining operating temperature during standby periods and start-up procedures must be considered. The effects of thermal cycling must be determined. We can be pleased with the results reported thus far, but we must recognize that a major portion of the work remains to be done before practical high-temperature batteries will be available.

References and Notes

1. W. Mitchell, Jr., Ed., *Fuel Cells* (Academic Press, New York, 1963); K. R. Williams, Ed., *An Introduction to Fuel Cells* (Elsevier, New York, 1966); H. A. Liebhafsky and E. J. Cairns, *Fuel Cells and Fuel Batteries* (Wiley, New York, 1968).
2. See, for example, A. M. Moos and N. I. Palmer, *Proc. 21st Annu. Power Sources Conf.* **21**, 51 (1967); S. M. Chodosh, M. G. Rosansky, B. E. Jagid, *ibid.*, p. 103; C. E. Kent, *ibid.*, p. 106; A. Charkey and G. A. Dalin, *Proc. 20th Annu. Power Sources Conf.* **20**, 79 (1966).
3. G. W. Vinal, *Storage Batteries* (Wiley, New York, 1955).
4. P. C. Milner and U. B. Thomas, *Advan. Electrochem. Electrochem. Eng.* **5** (1967).
5. R. Jasinski, *High-Energy Batteries* (Plenum Press, New York, 1967).
6. H. Shimotake and E. J. Cairns, in *Intersociety Energy Conversion Engineering Conference 1968 Record* (Institute of Electrical and Electronics Engineers, New York, 1968).
7. G. W. Vinal, *Primary Batteries* (Wiley, New York, 1950).
8. D. A. J. Swinkels, *J. Electrochem. Soc.* **113**, 6 (1966).
9. P. R. Shipps, *Proc. 20th Annu. Power Sources Conf.* **20**, 86 (1966); A. M. Moos and N. I. Palmer, *Proc. 21st Annu. Power Sources Conf.* **21**, 51 (1967).
10. C. E. Kent, *Proc. 21st Annu. Power Sources Conf.* **21**, 106 (1967).
11. G. J. Janz, *Molten Salts Handbook* (Academic Press, New York, 1967).
12. E. H. Hietbrink, J. J. Petrarts, D. A. J. Swinkels, G. M. Craig, *General Motors Company Technical Report Air Force Aero Propulsion Laboratory TR-67-89* (August 1967).
13. D. A. J. Swinkels, *IEEE (Inst. Elec. Electron. Eng.) Spectrum* **5**, 71 (May 1968).
14. ——, *J. Electrochem. Soc.* **114**, 812 (1967).
15. ——, *Electrochem. Tech.* **5**, 396 (1967).
16. E. J. Cairns, C. E. Crouthamel, A. K. Fischer, M. S. Foster, J. C. Hesson, C. E. Johnson, H. Shimotake, A. D. Tevebaugh, *Argonne Nat. Lab. Rep. No. 7316* (1968).
17. R. A. Rightmire and A. L. Jones, *Proc. 21st Annu. Power Sources Conf.* **21**, 42 (1967).
18. N. Weber and J. T. Kummer, *ibid.*, p. 37.
19. L. A. Heredy, M. L. Iverson, L. R. McCoy, R. D. Odenkamp, paper presented at High Energy Batteries Symposium, Los Angeles, December 1967; L. A. Heredy, personal communication.
20. H. Shimotake, G. L. Rogers, E. J. Cairns, paper presented at Electrochemical Society Meeting, Chicago, October 1967; see also *Extended Abstr. Battery Div.* **12**, 42 (1967).
21. H. Shimotake and E. J. Cairns, paper presented at Comité International de Thermodynamique et de Cinetique Electrochimiques Meeting of the International Union of Pure and Applied Chemistry, Detroit, September 1968; *Extended Abstr.*, p. 254.
22. H. Shimotake and E. J. Cairns, in preparation.
23. G. H. J. Broers and M. Schenke, *Fuel Cells*, G. J. Young, Ed. (Reinhold, New York, 1963), vol. 2, p. 6; G. H. J. Broers, in *Fuel Cells, A CEP Technical Manual* (American Institute of Chemical Engineers, New York, 1963).
24. B. S. Baker, L. G. Marianowski, J. Zimmer, G. Price, *Hydrocarbon Fuel Cell Technology*, B. S. Baker, Ed. (Academic Press, New York, 1965), p. 293; A. D. S. Tantram, A. C. C. Tseung, B. S. Harris, *ibid.*, p. 187.
25. H. Shimotake, G. L. Rogers, E. J. Cairns, *Ind. Eng. Chem. Process Design Develop.* **8**, 51 (1969).
26. E. J. Cairns and H. Shimotake, paper presented at American Chemical Society Meeting, Chicago, September 1967, Abstr. No. L-70; *Preprints Pap. Presented Div. Fuel Chem.* **11** (3), 321 (1967); *Advan. Chem. Ser.*, in press.
27. U.S. Department of Commerce, *The Automobile and Air Pollution: A Program for Progress*, Report of the Panel on Electrically Powered Vehicles (October 1967).
28. R. E. Salathe, J. O. Smith, J. P. Gallagher, P. L. Terry, J. Kozloff, L. F. Athearn, *Proc. 21st Annu. Power Sources Conf.* **21**, 19 (1967); G. E. Evans, *ibid.*, p. 32.
29. E. M. Morse, *Proc. 19th Annu. Power Sources Conf.* **19**, 109 (1965); S. M. Chodosh, E. G. Katsoulis, M. G. Rosansky, in *Proceedings of the Intersociety Energy Conversion Engineering Conference* (American Institute of Aeronautics and Astronautics, New York, 1966).
30. D. R. Turner, W. E. Howden, T. Okinaka, E. J. McHenry, in *Power Sources 1966*, D. H. Collins, Ed. (Pergamon, New York, 1957).
31. G. A. Dalin and M. Sulkes, *Proc. 20th Annu. Power Sources Conf.* **20**, 120 (1966).
32. H. F. Bauman, *ibid.*, p. 73.
33. Work performed under the auspices of the U.S. Atomic Energy Commission. We thank G. L. Rogers and J. Peck for their experimental assistance, and A. D. Tevebaugh and R. C. Vogel for encouragement and support. Mrs. E. J. Hathaway provided editorial assistance.